Lee Hyunju (Orcid ID: 0000-0003-2389-7183)
Park Hee Kyung (Orcid ID: 0000-0001-6339-0059)

Accepted Article

# Detecting amyloid-$\beta$ positivity using regions of interest from structural MRIs

Jeongyoung Hwang[1], Hee Kyung Park[2,3], Hai-jeon Yoon[4], Jee Hyang Jeong[2,†], Hyunju Lee[1,5,†], for the Alzheimer's Disease Neuroimaging Initiative*

[1] *Artificial Intelligence Graduate School, Gwangju Institute of Science and Technology, Gwangju 61005, South Korea*
[2] *Department of Neurology, College of Medicine, Ewha Womans University, Seoul, 07804, South Korea*
[3] *Division of Psychiatry, Department of mental health care of older people, University College London, London*
[4] *Department of Nuclear medicine, College of Medicine, Ewha Womans University, Seoul, 07804, South Korea*
[5] *School of Electrical Engineering and Computer Science, Gwangju Institute of Science and Technology, Gwangju 61005, South Korea*
[†] *Corresponding author, Email:* jjeong@ewha.ac.kr (J.H.J.); hyunjulee@gist.ac.kr (H.J.L.)

**Data used in the preparation of this article were obtained from the Alzheimer's Disease Neuroimaging Initiative (ADNI) database (www.loni.ucla.edu/ADNI). As such, the investigators within the ADNI contributed to the design and implementation of ADNI and/or provided data but did not participate in analysis or writing of this report. Complete listing of ADNI investigators is available at http://adni.loni.ucla.edu/wp-content/uploads/how to apply/ADNI Authorship List.pdf*

**Correspondence** Jee Hyang Jeong, Department of Neurology, College of Medicine, Ewha Womans University, Seoul, 07804, South Korea; Hyunju Lee, Artificial Intelligence Graduate School, Gwangju Institute of Science and Technology, Gwangju, 61005, South Korea Email: jjeong@ewha.ac.kr (J.H.J.); hyunjulee@gist.ac.kr (H.J.L.)

**Funding information** This work was supported by the Bio & Medical Technology Development Program of NRF funded by the Korean government (MSIT) (NRF-2018M3C7A1054935) and Institute of Information communications Technology Planning Evaluation (IITP) grant funded by the Korea government (MSIT) [No.2019-0-01842, Artificial Intelligence Graduate School Program (GIST)].

## Abstract

**Background:** Alzheimer's disease (AD) is the most common type of dementia. Amyloid-β (Aβ) positivity is the main diagnostic marker for AD. Aβ positron emission tomography and cerebrospinal fluid are widely used in the clinical diagnosis of AD. However, these methods only assess the concentrations of Aβ and the accessibility of these methods is thus relatively limited compared with structural magnetic resonance imaging (sMRI).

**Methods:** We investigated whether regions of interest (ROIs) in sMRIs can be used to predict Aβ positivity for samples with normal cognition (NC), mild cognitive impairment (MCI) and dementia. We obtained 846 Aβ negative (Aβ-) and 865 Aβ positive (Aβ+) samples from the Alzheimer's Disease Neuroimaging Initiative database. To predict which samples are Aβ+, we built five machine learning models using ROIs and apolipoprotein E (APOE) genotypes as features. To test the performance of the machine learning models, we constructed a new cohort containing 97 Aβ- and 81 Aβ+ samples.

**Results:** The best performing machine learning model combining ROIs and APOE had an accuracy of 0.798, indicating that it can help predict Aβ+. Furthermore, we searched ROIs that could aid our prediction and discovered that an average left entorhinal cortical region (L-ERC) thickness is an important feature. We also noted significant differences in L-ERC thickness between the Aβ- and Aβ+ samples even in the same diagnosis of NC, MCI, and dementia.

**Conclusions:** Our findings indicate that ROIs from sMRIs along with APOE can be used as an initial screening tool in the early diagnosis of AD.

## KEYWORDS

Alzheimer's disease, amyloid-β, sMRI, machine learning, left entorhinal cortical region

## Running Title

This article has been accepted for publication and undergone full peer review but has not been through the copyediting, typesetting, pagination and proofreading process which may lead to differences between this version and the Version of Record. Please cite this article as doi: 10.1111/ene.15775

This article is protected by copyright. All rights reserved.

Accepted Article



## 1. INTRODUCTION

Dementia, a progressive neurodegenerative brain disorder, is characterized by intellectual and cognitive decline [1], including Alzheimer's disease (AD), vascular dementia, and frontotemporal dementia. AD is the most common type of dementia and occurs in 60 to 80% of all patients with dementia [2]. The annual incidence of AD increases with age, showing 0.4%, 3.2%, and 7.6% for age 65 to 74, age 75 to 84, and age 85 and older, respectively [3].

It is challenging to identify the mechanisms underlying AD. However, the accumulation of amyloid-β (Aβ) plaques in the brain is suggested to be a major diagnostic marker of AD [4,5]. There exist representative methods for measuring Aβ positivity: positron emission tomography (PET) with $^{18}$F-florbetapir [6,7], $^{18}$Fflorbetaben ($^{18}$F-FBB) [8], and $^{18}$F-flutemetamol [9] is one method, while quantification of Aβ plaque load by measuring Aβ concentrations in cerebrospinal fluid (CSF) is another [10]. Some studies have also predicted Aβ positivity using structural magnetic resonance imaging (sMRI) and apolipoprotein E (APOE) genotypes [11,12]; these studies demonstrated that the predictive power for Aβ positivity in individuals with mild cognitive impairment (MCI) improved when sMRI and APOE genotypes were used together. Considering that sMRI has been performed with other diseases or injuries in clinics, the prediction of Aβ positivity using sMRI can be used as an initial screening tool for AD diagnosis.

In this study, to predict Aβ positivity, we constructed machine learning models using sMRI from two cohorts comprising normal cognition (NC), MCI, and dementia samples. The first cohort was the Ewha Womans (EW) cohort comprising 178 patients from the Ewha Womans University Mokdong Hospital and Ewha Womans University Seoul Hospital. The second cohort was obtained from the Alzheimer's Disease Neuroimaging Initiative (ADNI) database [13]. However, because the number of samples in the EW cohort was much smaller than the number of regions of interest (ROIs) from sMRI, ADNI was used for constructing the training models and the EW cohort was tested in terms of the Aβ classification process. Moreover, two APOE single nucleotide polymorphisms (SNPs) (rs429358 and rs7412) were used together with sMRI to increase the performance. We then performed permutation feature importance [14] using the best performing machine learning model to determine, from the sMRIs, the ROIs that greatly influenced Aβ positivity prediction. Finally, we identified ROIs that showed significant differences in Aβ accumulation across all cohorts and diagnoses of NC, MCI, and AD.

14681331, ja, Downloaded from https://onlinelibrary.wiley.com/doi/10.1111/ene.15775 by University Of Southern California, Wiley Online Library on [27/03/2023]. See the Terms and Conditions (https://onlinelibrary.wiley.com/terms-and-conditions) on Wiley Online Library for rules of use; OA articles are governed by the applicable Creative Commons License

Accepted Article

## 2. MATERIALS

### 2.1. EW cohort

We newly constructed the EW cohort by collecting data on $^{18}$F-FBB PET scanning, T1-weighted sMRI, and APOE genotypes of 178 subjects between June 2018 and July 2021 from the memory disorder clinic in Ewha Womans University Mokdong Hospital and Ewha Womans University Seoul Hospital. The acquisition methods of these data sets are described in Supplementary Section 1. The included subjects satisfied the following criteria: (1) aged between 50 and 90 years, (2) presence on the Alzheimer's continuum modified from the National Institute on Aging and Alzheimer's Association research framework in 2018 [15], (3) presence of a reliable informant, (4) the ability to read and write, and (5) provided written informed consent.

To distinguish the patient's diagnostic status, global cognition was assessed using the Korean-Mini-Mental Status Examination (K-MMSE)[16], global clinical dementia rating (CDR), sum of boxes of CDR, and a detailed neuropsychological battery of Seoul Neuropsychological Screening Battery-II [17]. To determine the Aβ positivity of the subjects, two expert PET readers visually judged the $^{18}$F-FBB PET PET data, with all clinical information masked [18,19]. The tracer uptake in four cortical regions (lateral temporal cortex, frontal cortex, parietal cortex, and posterior cingulate cortex/precuneus) was evaluated using the regional cortical tracer uptake (RCTU) system (1 = no uptake, 2 = moderate uptake, 3 = pronounced uptake). Next, the global uptake in the brain was evaluated using the brain amyloid plaque load system (1 = RCTU score 1 in each of the four brain regions, 2 = RCTU score 2 in any of the four brain regions and no RCTU score 3 in these regions, 3 = RCTU score 3 in at least one of the four brain regions). Finally, patients with PET scans with a brain amyloid plaque load score of 2 and 3 were designated as Aβ positive (Aβ+), whereas the others were distinguished as Aβ negative (Aβ-).

### 2.2. ADNI cohort

We downloaded data on sMRI, PET, and APOE genotypes from the ADNI website. We used the "UCSF Cross-Sectional FreeSurfer (4.3) (version 2015-11-2)" dataset, which contains brain structural information, and the "UC Berkeley-AV45 Analysis (version 2016-10- 17)" dataset for PET, which contains Aβ information. The Aβ- and Aβ+ cut off was 1.11 standard uptake value ratios normalized by the whole cerebellar reference region [20]. We used the "ApoE-Results (version 2013-05- 14)" dataset that contains information on the two SNPs rs429358 and rs7412.

The ADNI database comprises data from the same subject collected multiple times. Because we used the ADNI database for training a model, all the data from each subject were used. Finally, we used 1,711 samples with all information on sMRI, PET, and APOE in the ADNI cohort.

### 2.3. EW and ADNI + EW datasets for a predictive model

We constructed two datasets to build and evaluate a predictive model that classifies Aβ+ and Aβ- samples. The first dataset was called the EW dataset; samples in this cohort were divided into 60%, 20%, and 20% as training, validation, and test sets, respectively, for five-fold cross-validation (CV). The second dataset was called the ADNI + EW dataset, where all samples in the ADNI cohort were used for the training set; the samples in the training and validation datasets of the EW dataset in each CV were used as the validation set; and samples in the test set of the EW dataset in each CV were used as the test set. Because the test sets in the EW and ADNI + EW datasets were same, it was possible to check whether the ADNI cohort is beneficial in improving the classification performance of the EW cohort.

14681331, ja, Downloaded from https://onlinelibrary.wiley.com/doi/10.1111/ene.15775 by University Of Southern California, Wiley Online Library on [27/03/2023]. See the Terms and Conditions (https://onlinelibrary.wiley.com/terms-and-conditions) on Wiley Online Library for rules of use; OA articles are governed by the applicable Creative Commons License

Accepted Article

### 2.4. sMRI preprocessing

For the EW cohort, ROIs were extracted from sMRIs using the FreeSurfer (6.0) software package (http:// surfer.nmr.mgh.harvard.edu). For both the ADNI and EW cohorts, a total of 311 ROIs, including cortical volume, mean cortical thickness, cortical thickness standard deviation, and subcortical volume and surface area, were used.

Brain volume and thickness decrease with age, and this can be a confounding factor biasing the neuroimaging analysis of AD [21,22]. Thus, the performance of a predictive model can be improved by eliminating this confounding factor [23]. Using generalized linear regression [24], we removed two confounders of age and cohort (ADNI or EW cohort) from sMRI data in the ADNI + EW dataset, and a confounder of age from sMRI data in ADNI and EW datasets (see Supplementary Section 2).

### 2.5. Mapping the APOE genotype to SNPs

Because APOE is involved in Aβ binding, clearance, and brain synaptic function, any alterations in the APOE genotype can cause Aβ plaque accumulation in the cerebral cortex [25,26]. In particular, APOE ϵ4 is an important biomarker for predicting Aβ [27]. Therefore, we used the two SNPs rs429358 and rs7412; they represent six genotypes of APOE [28].

14681331, ja, Downloaded from https://onlinelibrary.wiley.com/doi/10.1111/ene.15775 by University Of Southern California, Wiley Online Library on [27/03/2023]. See the Terms and Conditions (https://onlinelibrary.wiley.com/terms-and-conditions) on Wiley Online Library for rules of use; OA articles are governed by the applicable Creative Commons License

Accepted Article

## 3. METHODS

### 3.1. Machine learning methods for the prediction of Aβ positivity

For the prediction of Aβ positivity, a total of five machine learning methods [logistic regression (LR), decision tree (DT), random forest (RF), support vector machine (SVM), and XGBoost (XGB) [29] were constructed, and the performances of these methods were measured with five-fold CV using accuracy (ACC), f1-score (F1), area under the receiver operating characteristic curve (AUC), and Matthews correlation coefficient (MCC) [30]. The set of hyperparameter values of the five machine learning models is described in Supplementary Section 3.

### 3.2. Feature selection methods for identifying ROIs related to Aβ positivity

After constructing the models for predicting Aβ positivity, we assessed the ROIs of the sMRI that contribute to the classification of the Aβ+ sample. First, we selected a model with the highest test MCC among the five machine learning methods. Next, for each ROI, permutation-based feature importance was calculated by estimating decreases in performance by randomly shuffling the values of a feature [14]. For each fold of the five-fold CV, the permutation-based feature importance was calculated 100 times to reduce variance in prediction errors; then, the highest-scoring 20 of 311 ROIs were selected. Third, the ROIs that were ranked in the top 20 in at least two folds of the five-fold CV were selected.

We further refined the ROIs related to Aβ positivity among the important ROIs from the classification of Aβ+ samples using machine learning. The t-test was performed to assess differences between the Aβ+ and Aβsamples for each diagnosis of NC, MCI, and dementia for all of the samples in the EW, ADNI, and ADNI + EW datasets. ROIs with a p-value of $< 0.1$ were considered to be related to Aβ accumulation.

14681331, ja, Downloaded from https://onlinelibrary.wiley.com/doi/10.1111/ene.15775 by University Of Southern California, Wiley Online Library on [27/03/2023]. See the Terms and Conditions (https://onlinelibrary.wiley.com/terms-and-conditions) on Wiley Online Library for rules of use; OA articles are governed by the applicable Creative Commons License

Accepted Article

# 4. RESULTS

## 4.1. Datasets

**Table 1.** Characteristics of the patients in the EW and ADNI cohorts.

| Properties | EW cohort | | | ADNI cohort | | | p-values of two cohorts[a] |
|---|---|---|---|---|---|---|---|
| Number of samples | 97 | 81 | - | 846 | 865 | - | - |
| NC/MCI/Dementia | 37/46/14 | 5/46/30 | <1e-05* | 421/389/36 | 184/435/246 | <1e-05* | 0.001* |
| APOE non-ϵ4/APOE ϵ4 | 86/11 | 32/49 | <1e-05* | 684/162 | 329/536 | <1e-05* | 0.079 |
| Male/Female | 61/36 | 47/34 | 0.612 | 459/387 | 452/413 | 0.435 | 0.070 |
| Age (years) | 69.84±7.28 | 73.28±7.23 | 0.002* | 73.01±7.67 | 74.84±7.11 | <1e-05* | 2e-05* |
| Education (years) | 10.63±4.61 | 10.12±4.81 | 0.476 | 16.54±2.52 | 15.95±2.77 | <1e-05* | <1e-05* |
| MMSE[b] (score) | 26.37±4.22 | 22.83±5.08 | <1e-05* | 28.51±2.08 | 26.22±3.80 | <1e-05* | <1e-05* |
| CDRSB | 1.91±2.70 | 3.51±2.71 | 1e-04* | 0.79±1.22 | 2.35±2.58 | <1e-05* | <1e-05* |

Note: p-values for the characteristics based on diagnosis, APOE, and sex were calculated using the two-sample Chi-square test. For the MMSE, age, education, and CDRSB, the mean ± standard deviation values have been shown, and the p-values were calculated using the two-sample t-test. * indicates that the p-value is < 0.05. In the ADNI cohort, five and thriteen samples did not have values for MMSE and CDRSB, respectively.
Abbreviations: AD, Alzheimer's Disease; Aβ-, Aβ negative; Aβ+, Aβ positive; EW, Ewha Womans; ADNI, Alzheimer's Disease Neuroimaging Initiative; NC, normal cognition; MCI, mild cognitive impairment; APOE, apolipoprotein E; MMSE, Mini-Mental State Examination; CDRSB, Clinical Dementia Rating sum of boxes
[a]The t-test and two-sample Chi-square test were performed to assess differences between the EW and ADNI cohorts.
[b]The EW and ADNI cohorts were measured by Korean-MMSE and MMSE, respectively

The characteristics of the patients in the EW and ADNI cohorts are summarized in Table 1. Table 1 shows significant differences in age, education, MMSE, and CDRSB between the EW and ADNI cohorts. The adjustment for the differences in age and the cohort categories was performed using generalized linear regression in Section 2.4. As the number of NC samples in EW is relatively smaller than that in ADNI, MMSE and CDRSB values were different accordingly.

## 4.2. Aβ+ classification results

**Table 2.** Prediction of Aβ positivity measured as ACC, F1, AUC, and MCC in the EW and ADNI + DW datasets.

| Features | Models | EW dataset ACC | F1 | AUC | MCC | ADNI + EW dataset ACC | F1 | AUC | MCC |
|---|---|---|---|---|---|---|---|---|---|
| SNP | DT | **0.759±0.036** | **0.705±0.048** | **0.770±0.026** | **0.516±0.070** | 0.775±0.016 | 0.719±0.027 | 0.755±0.037 | 0.560±0.042 |
| sMRI | DT | 0.545±0.064 | 0.513±0.080 | 0.542±0.053 | 0.095±0.135 | 0.714±0.077 | 0.688±0.108 | 0.732±0.098 | 0.436±0.155 |
| | LR | 0.680±0.065 | 0.655±0.074 | 0.697±0.062 | 0.364±0.128 | 0.702±0.064 | 0.693±0.095 | 0.804±0.064 | 0.423±0.144 |
| | RF | 0.641±0.087 | 0.581±0.093 | 0.708±0.050 | 0.272±0.174 | 0.674±0.030 | 0.684±0.051 | 0.781±0.056 | 0.384±0.070 |
| | SVM | 0.641±0.038 | 0.520±0.091 | 0.695±0.044 | 0.294±0.095 | 0.697±0.080 | 0.686±0.114 | 0.811±0.067 | 0.422±0.170 |
| | XGB | 0.663±0.056 | 0.588±0.092 | 0.665±0.021 | 0.312±0.119 | 0.696±0.097 | 0.708±0.101 | 0.798±0.081 | 0.436±0.186 |
| | Average | 0.634±0.079 | 0.571±0.101 | 0.661±0.078 | 0.268±0.161 | 0.697±0.074 | 0.692±0.097 | 0.785±0.080 | 0.420±0.152 |
| sMRI + SNP | DT | 0.664±0.125 | 0.604±0.164 | 0.659±0.145 | 0.323±0.259 | 0.787±0.026 | 0.770±0.032 | 0.822±0.027 | 0.576±0.049 |
| | LR | 0.686±0.068 | 0.646±0.107 | 0.758±0.078 | 0.375±0.134 | 0.792±0.057 | 0.772±0.067 | 0.847±0.036 | 0.586±0.110 |
| | RF | 0.674±0.048 | 0.596±0.060 | 0.753±0.042 | 0.340±0.098 | 0.775±0.035 | 0.770±0.050 | 0.843±0.057 | 0.566±0.077 |
| | SVM | 0.658±0.061 | 0.581±0.111 | 0.713±0.056 | 0.314±0.118 | 0.759±0.065 | 0.743±0.085 | 0.846±0.042 | 0.524±0.141 |
| | XGB | 0.725±0.057 | 0.679±0.068 | 0.753±0.044 | 0.449±0.110 | **0.798±0.041** | **0.786±0.060** | **0.857±0.060** | **0.613±0.086** |
| | Average | 0.681±0.080 | 0.621±0.114 | 0.727±0.091 | 0.360±0.163 | 0.782±0.049 | 0.768±0.063 | 0.843±0.048 | 0.573±0.102 |

All values in the table have been expressed as mean ± standard deviation. Boldface represents the best performance of each dataset.
Abbreviations: ACC, accuracy; F1, f1-score; AUC, area under the receiver operating characteristic curve; MCC, Matthews correlation coefficient; sMRI, structural magnetic resonance imaging; SNP, single nucleotide polymorphism; DT, decision tree; LR, logistic regression; RF, random forest; SVM, support vector machine; XGB, XGBoost.

Table 2 shows the performances of the classification of the Aβ+ samples as per five machine learning methods using the EW and ADNI + EW datasets. Compared with the EW dataset, the average performances of the five methods increased in the ADNI + EW dataset. When both sMRI and SNPs were used as features, on average, a 0.101, 0.147, 0.116, and 0.213 increase was noted in the ACC, F1, AUC, and MCC, respectively. Similarly, when sMRI was

14681331, ja, Downloaded from https://onlinelibrary.wiley.com/doi/10.1111/ene.15775 by University Of Southern California, Wiley Online Library on [27/03/2023]. See the Terms and Conditions (https://onlinelibrary.wiley.com/terms-and-conditions) on Wiley Online Library for rules of use; OA articles are governed by the applicable Creative Commons License

used as a feature, the average performance of the ADNI + EW dataset was higher than that of the EW dataset. In Table 2, the performances of all 40 cases (five classification methods × four metrics) increased when the ADNI cohort was used for training in the ADNI + EW dataset. This performance improvement indicates that the EW cohort used in this study has a similar distribution to the widely used ADNI cohort and that a large number of training samples is helpful for a more accurate classification of Aβ+ samples.

When the cases using sMRI and two SNPs as multimodalities were compared with the cases using sMRI as a single modality, average increases of 0.047, 0.050, 0.066, and 0.092 were noted for ACC, F1, AUC, and MCC, respectively, in the EW dataset, and 0.085, 0.076, 0.058, and 0.153, respectively, in the ADNI + EW dataset. When both sMRI and SNP were used as features, all performance metrics were higher, except for F1 of LR, when using sMRI only.

In the EW dataset, the performances of all methods that used only sMRI or the multimodalities of SNP and sMRI were lower than those of the methods using SNPs. However, in the ADNI + EW dataset, although the models that used SNPs as features exhibited better performances than the models that used sMRI as features, the models that used both sMRI and SNPs as features outperformed the models that used single modalities (SNPs or sMRI). In addition, when sMRI was used as a single modality feature, the average performances of the five machine learning models were 0.697, 0.692, 0.785, and 0.420 for ACC, F1, AUC, and MCC, respectively, indicating that the Aβ samples could be distinguished using sMRI. Our results indicate that the SNPs rs429358 and rs7412 are more important than sMRI as biomarkers for judging Aβ positivity; however, if the number of datasets is sufficient, sMRI can be a major biomarker that can judge Aβ positivity; moreover, the classification of Aβ+ samples can be improved by combining sMRI and SNPs.

Taken together, the models that used sMRI and SNPs as features in the ADNI + EW dataset outperformed all of the other models used for the classification of the Aβ+ samples. In particular, the XGBoost method showed the highest performances of 0.798 ± 0.041, 0.786 ± 0.060, 0.857 ± 0.060, and 0.613 ± 0.086 in terms of ACC, F1, AUC, and MCC, respectively.

For comparison, we measured the prediction performance of the ADNI dataset by dividing 60%, 20%, and 20% of the 1,033 non-duplicated subjects into the training set, validation set, and test set, respectively, in the five-fold CV. The performance of the five machine learning models using the ADNI dataset are described in Supplementary Table 1. The DT method had the highest ACC and MCC values of 0.733 and 0.469, respectively, but they were lower than that in the ADNI + EW dataset.

### 4.3. Classification of Aβ+ samples in the diagnosis groups using the ADNI + EW and ADNI datasets

Table 1 shows that the ratios of diagnosis between the Aβ- and Aβ+ samples were significantly different ($p < 1e{-}05$). While the ratios of the Aβ- and Aβ+ samples were similar for MCI, they were different for NC and dementia because AD is the most common type of dementia. Here, we additionally used the ADNI dataset because the number of samples in some diagnostic categories of the ADNI + EW dataset are small, such as five samples in Aβ+ NC. Therefore, we performed the following procedure to check whether the discriminate power of the Aβ+ samples in Table 2 was caused by the patient's diagnosis.

First, for each dataset, we selected a model that had the highest test MCC values among the five machine learning methods when both SNPs and sMRI were used. For the ADNI + EW and ADNI datasets, the selected model was XGBoost and DT, respectively.

Accepted Article

14681331, ja, Downloaded from https://onlinelibrary.wiley.com/doi/10.1111/ene.15775 by University Of Southern California, Wiley Online Library on [27/03/2023]. See the Terms and Conditions (https://onlinelibrary.wiley.com/terms-and-conditions) on Wiley Online Library for rules of use; OA articles are governed by the applicable Creative Commons License

Second, the prediction of Aβ positivity for all the test samples was obtained using the five-fold CV results of the selected models.

**Table 3.** Accuracy of the prediction of Aβ positivity of each diagnosis of NC, MCI, and dementia for the ADNI + EW and ADNI datasets.

| Diagnosis | ADNI + EW dataset | | | ADNI dataset | | |
|---|---|---|---|---|---|---|
| | All | Aβ- | Aβ+ | All | Aβ- | Aβ+ |
| NC | 0.833 (35/42) | 0.865 (32/37) | 0.600 (3/5) | 0.714 (432/605) | 0.808 (340/421) | 0.500 (92/184) |
| MCI | 0.750 (69/92) | 0.696 (32/46) | 0.804 (37/46) | 0.718 (592/824) | 0.799 (311/389) | 0.646 (281/435) |
| Dementia | 0.864 (38/44) | 0.714 (10/14) | 0.933 (28/30) | 0.816 (230/282) | 0.861 (31/36) | 0.809 (199/246) |

Abbreviations: Aβ-, Aβ negative; Aβ+, Aβ positive; EW, Ewha Womans; ADNI, Alzheimer's Disease Neuroimaging Initiative; NC, normal cognition; MCI, mild cognitive impairment.

**Figure 1.** Boxplots of the normalized left entorhinal cortical thickness average are shown for Aβ+ (in blue) and Aβ- (in red) samples in the ADNI + EW dataset (A), the ADNI dataset (B), and the EW dataset (C). Abbreviations: Aβ-, Aβ negative; Aβ+, Aβ positive; NC, normal cognition; MCI, mild cognitive impairment.

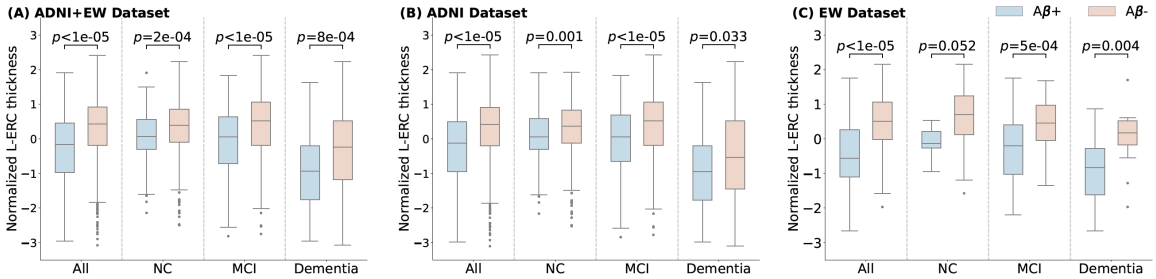


Table 3 shows the ACC of the predictions of Aβ positivity for the three diagnosis categories in each dataset, where a threshold for positive or negative prediction is 0.5. In the ADNI + EW dataset, the ACC of the Aβ+ NC sample was low as 60.0%, but the ACC of the Aβ- dementia sample was 71.4%, which was similar to that of the MCI samples. Supplementary Figure 1 shows that when the thresholds for predicting positive or negative Aβ were 0.4 and 0.6, the ACCs of each category were also similar with those using a threshold of 0.5. These results indicate that the prediction performance of the XGBoost method was not biased toward the patient's diagnosis.

In the ADNI dataset, of 282 dementia samples, 36 were Aβ- and 86.1% were correctly predicted, which had a higher ACC than that of Aβ+. However, the ACC of the Aβ+ NC sample was as low as 50.0%. Furthermore, when the threshold for deciding positive or negative Aβ was 0.4, ACCs of Aβ+ NC and Aβ- NC samples were 0.625 and 0.682, respectively (Supplementary Figure 2). These results support that the prediction of Aβ positivity was not biased toward the patient's diagnosis.

In addition, based on the results in Table 3, we calculated post-test probabilities of a sample being Aβ+ when it was predicted to be Aβ+. For the ADNI + EW dataset, a pre-test probability was 0.455, and a post-test probability increased to 0.747 with a positive likelihood ratio of 3.541. Similarly, for the ADNI dataset, the pretest probability was 0.506, and the post-test probability increased to 0.777 with the positive likelihood ratio of 3.411.

**Figure 2.** Visualization of the thickness of the left entorhinal cortical region in the EW cohort. "Mean" is the average of all the subjects in the Aβ+ or Aβ- groups in a given diagnosis category, whereas "Value" is the actual value of the subject that is the closest to the mean. Abbreviations: Aβ-, Aβ negative; Aβ+, Aβ positive; NC, normal cognition; MCI, mild

Accepted Article

14681331, ja, Downloaded from https://onlinelibrary.wiley.com/doi/10.1111/ene.15775 by University Of Southern California, Wiley Online Library on [27/03/2023]. See the Terms and Conditions (https://onlinelibrary.wiley.com/terms-and-conditions) on Wiley Online Library for rules of use; OA articles are governed by the applicable Creative Commons License

cognitive impairment. Abbreviations: Aβ-, Aβ negative; Aβ+, Aβ positive; NC, normal cognition; MCI, mild cognitive impairment.

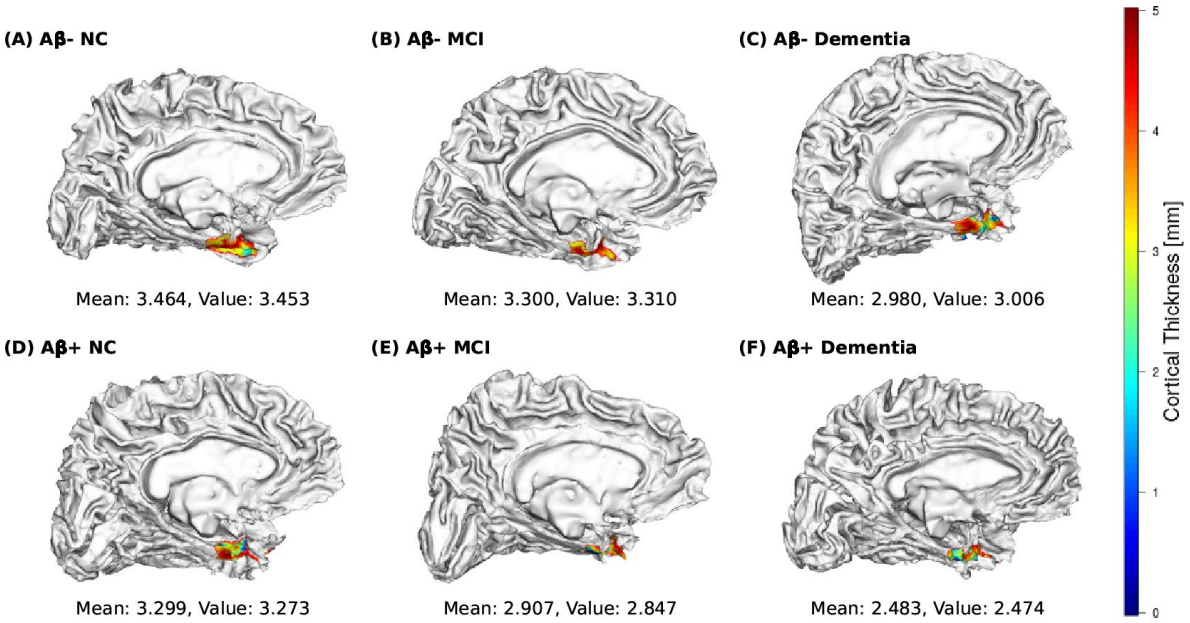


### 4.4. ROIs related to the classification of Aβ+ samples

To identify the ROIs of the sMRI contributing to the classification of Aβ+ samples in the prediction models, permutation-based feature importance was calculated for each ROI using the XGBoost method. Supplementary Table 2 shows ROIs that were selected as important features in the classification of Aβ+ samples. The measurement of permutation-based feature importance identified 12 important ROIs that ranked within the top 20 in at least 2 CVs of the five-fold CVs. Among the 12 ROIs, significant differences (p-value < 0.1) between the Aβ- and Aβ+ samples were noted in most ROIs, regardless of cohorts. However, several ROIs did not show significant differences in the dementia category of the ADNI and ADNI + EW datasets and the NC category of the EW dataset.

Among the 12 important ROIs in the classification of Aβ positivity, five ROIs had significant differences (p-value < 0.1 in the t test) between the Aβ- and Aβ+ samples in all diagnoses for at least one dataset (Table 4).

Among the five ROIs, four were related to Aβ only in a specific cohort or diagnosis. However, the left entorhinal cortical thickness average (L-ERC thickness) showed a significant difference (p-value < 0.1) between the Aβand Aβ+ samples in all diagnoses and all datasets.

**Table 4.** The five ROIs of sMRI contributing to the classification of Aβ+ samples with statistical significance.

| Datasets | ROIs | Measures | # of CVs[a] | All[b] | NC[c] | MCI[d] | Dementia[e] |
|---|---|---|---|---|---|---|---|
| ADNI and EW cohorts | Left Entorhinal | Cortical Thickness Average | 2 | <1e-05 | 2e-04 | <1e-05 | 8e-04 |
| | Left Medial Orbitofrontal | Cortical Thickness Average | 2 | <1e-05 | 0.004 | <1e-05 | **0.848** |
| | Right Entorhinal | Cortical Thickness Average | 2 | <1e-05 | 9e-04 | <1e-05 | 0.025 |
| | Right Entorhinal | Cortical Volume | 2 | <1e-05 | 3e-04 | <1e-05 | 0.005 |
| | Right Pars Orbitalis | Cortical Volume | 2 | <1e-05 | 0.057 | 2e-05 | 0.056 |
| ADNI cohort | Left Entorhinal | Cortical Thickness Average | 2 | <1e-05 | 0.001 | <1e-05 | 0.033 |
| | Left Medial Orbitofrontal | Cortical Thickness Average | 2 | <1e-05 | 0.017 | <1e-05 | **0.273** |
| | Right Entorhinal | Cortical Thickness Average | 2 | <1e-05 | 0.004 | <1e-05 | **0.232** |
| | Right Entorhinal | Cortical Volume | 2 | <1e-05 | 4e-04 | <1e-05 | 0.090 |
| | Right Pars Orbitalis | Cortical Volume | 2 | <1e-05 | **0.109** | 3e-05 | **0.474** |
| EW cohort | Left Entorhinal | Cortical Thickness Average | 2 | <1e-05 | 0.052 | 5e-04 | 0.004 |

Accepted Article

14681331, ja, Downloaded from https://onlinelibrary.wiley.com/doi/10.1111/ene.15775 by University Of Southern California, Wiley Online Library on [27/03/2023]. See the Terms and Conditions (https://onlinelibrary.wiley.com/terms-and-conditions) on Wiley Online Library for rules of use; OA articles are governed by the applicable Creative Commons License

| | | | | | | |
|---|---|---|---|---|---|---|
| Left Medial Orbitofrontal | Cortical Thickness Average | 2 | <1e-05 | 0.073 | 0.003 | 0.024 |
| Right Entorhinal | Cortical Thickness Average | 2 | <1e-05 | 0.065 | 0.005 | 0.053 |
| Right Entorhinal | Cortical Volume | 2 | 1e-05 | **0.389** | 0.040 | 0.024 |
| Right Pars Orbitalis | Cortical Volume | 2 | 0.002 | 0.061 | **0.225** | 0.017 |

Note: p-values > 0.1 are presented in bold
Abbreviations: NC, normal cognition; MCI, mild cognitive impairment.
[a]The number of cross-validation (CV) folds, where the ROI is in the top 20 in the permutation feature importance calculation.
[b] P -values of the t-test for the mean difference between all Aβ- and all Aβ+ samples
[c] P -values of the t-test for the mean difference between Aβ- NC and Aβ+ NC samples.
[d] P -values of the t-test for the mean difference between Aβ- MCI and Aβ+ MCI samples.
[e] P -values of the t-test for the mean difference between Aβ- dementia and Aβ+ dementia samples.

### 4.5. Cortical thickness of the left entorhinal region is related to the accumulation of Aβ

Figure 1 shows boxplots of normalized L-ERC thickness that was grouped based on Aβ positivity, Aβ negativity, and p-values of the t-test for the mean difference of normalized L-ERC thickness between the Aβ- and Aβ+ samples in all combinations of diagnoses and datasets. The normalized L-ERC thickness was thinner for Aβ+ samples than Aβ- samples, regardless of the datasets and the diagnosis of the sample. Figure 2 shows the left entorhinal region of sample subjects whose L-ERC thicknesses were closest to the mean of that for the samples of each diagnosis category and Aβ negativity or Aβ positivity in the EW cohort. Even if the diagnosis was the same, it could be seen that the L-ERC thickness of the Aβ+ samples was thinner than that of the Aβ- samples.

### 4.6. Associations of left entorhinal cortical thickness with APOE genotypes and age

We also conducted an experiment to see whether L-ERC was related to age and APOE genotypes with significant p-values between Aβ+ and Aβ- in Table 1. Figure 3 shows boxplots of normalized L-ERC thickness grouped by APOE genotypes and p-values of a t-test showing the mean difference of normalized L-ERC thickness between samples with APOE ϵ2/APOE ϵ3 and those with APOE ϵ4 in the EW, ADNI, and ADNI + EW datasets. For all three datasets, the p-values were significant (p-value < 0.1), which confirmed that the L-ERC thickness is related not only to Aβ accumulation but also to APOE genotypes.

**Figure 3.** Boxplots of the normalized average of the left entorhinal cortical thickness are shown for samples with ϵ4 (in blue) and samples with ϵ2 and ϵ3 (in red) in the ADNI + EW, ADNI, and EW datasets.

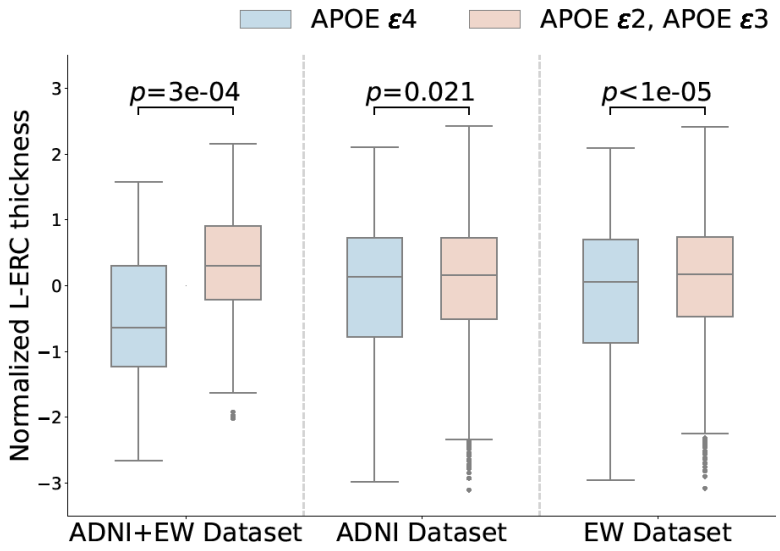


Accepted Article

14681331, ja, Downloaded from https://onlinelibrary.wiley.com/doi/10.1111/ene.15775 by University Of Southern California, Wiley Online Library on [27/03/2023]. See the Terms and Conditions (https://onlinelibrary.wiley.com/terms-and-conditions) on Wiley Online Library for rules of use; OA articles are governed by the applicable Creative Commons License

**Figure 4.** Correlation plots between the average of the left entorhinal cortical thickness (L-ERC thickness) and age. The bold red line is the regression line and the red zone is the 95% confidence interval.

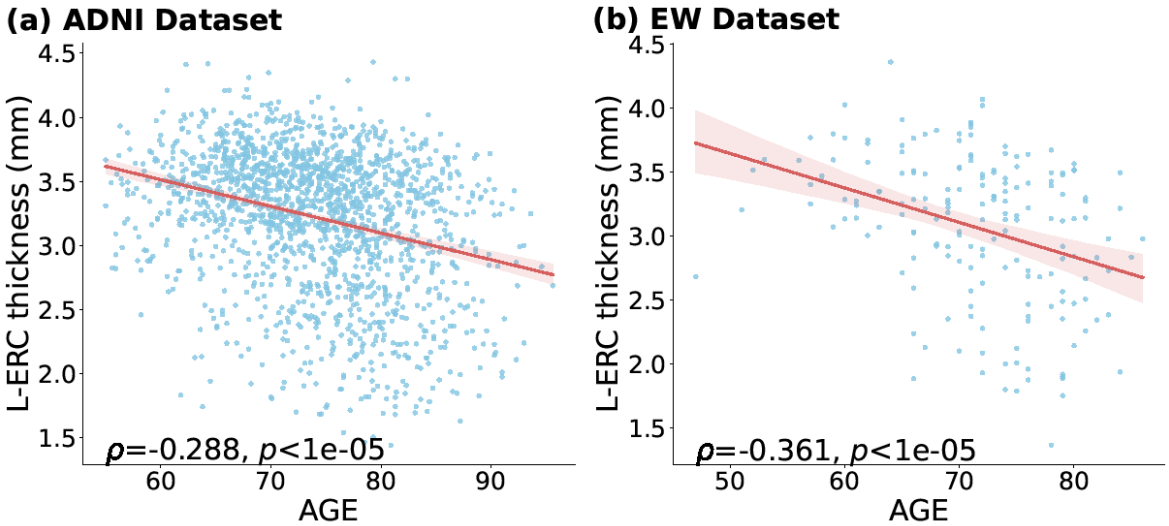


Figure 4 shows a negative correlation between L-ERC thickness and age with statistical significance for the ADNI and EW datasets, indicating that L-ERC thickness decreases as age increases. However, as a result of linear regression, the coefficient of the L-ERC thickness was -0.022 with a p-value of 0.963, and the p-value was ranked 306th out of 311, indicating that it is relatively less affected by age than other ROIs are. The experiment is detailed in Supplementary Section 4 and coefficients and p-values of all ROIs are provided in Supplementary Table 3.

Accepted Article

14681331, ja, Downloaded from https://onlinelibrary.wiley.com/doi/10.1111/ene.15775 by University Of Southern California, Wiley Online Library on [27/03/2023]. See the Terms and Conditions (https://onlinelibrary.wiley.com/terms-and-conditions) on Wiley Online Library for rules of use; OA articles are governed by the applicable Creative Commons License

Accepted Article

## 5. DISCUSSION

Although amyloid PET can determine AD positivity, it is usually practiced in clinics only when considerable cognition impairment is noted due to its high cost. CSF based methods are considered to reflect the level of amyloid in brain; however, their invasiveness often prevents their implementation to elderly adults. However, sMRI is a relatively more accessible approach. Thus, we constructed machine learning models to classify Aβ positivity using ROIs from sMRI in the ADNI cohort. Because the ADNI cohort contains a large number of samples, when it was used as the training data the prediction accuracy of the EW cohort was improved to approximately 0.7 compared to when part of EW cohort was used as training data (Table 2). This indicates that the machine learning classification model can be used across cohorts from different continents. Note that the ADNI data was collected in the United States and Canada while the EW data was collected in South Korea. When APOE genotypes were combined with sMRI, the accuracy reached 0.798 with XGB. Moreover, the accuracies from several machine learning classifiers exhibited 0.782 on average, similar to the highest accuracy score, indicating that the classification performance does not depend on classifiers. However, we may expect more improved accuracies if more complex models, such as deep learning approaches, can be used when the larger number of samples with AD diagnosis, sMRI, and APOE genotypes are available.

We also checked whether the prediction accuracy depends on the diagnosis of samples (Table 3). Previous studies showed that sMRI combined with clinical variables can be used to predict Aβ+ for MCIs with accuracies of around 0.8 [11, 12]. In our study, the prediction accuracies in MCI were 0.750 and 0.718 for the EW cohort and ADNI cohort, respectively. Although we cannot directly compare these accuracies due to the differences in the cohorts, our study could confirm the applicability of sMRI to the prediction of Aβ pathology in MCI. Among the dementia group, accuracies in samples with Aβ+ were high as 0.933 and 0.809 for the EW cohort and ADNI cohort, respectively. Encouragingly, accuracies in samples with Aβ- were 0.714 and 0.861 for the EW dataset and the ADNI dataset, respectively, showing that our approach can differentiate different types of dementia. In the NC samples, the accuracies were 0.833 and 0.714 for the EW cohort and the ADNI cohort, respectively, and Aβ- samples seem to be more correctly predicted than Aβ+ samples. However, when we used different thresholds for predicting positive or negative samples, prediction accuracies of Aβ+ samples can be improved, although the overall accuracies decreased slightly (Supplementary Figures 1 and 2). This result illuminates the possibilities of early diagnosis of Aβ+ for NC.

Table 1 shows that the distributions of diagnosis categories, years of education, and MMSE and CDRSB values were different between the EW and ADNI cohorts. In our prediction model, we did not take these feature values into account because we focused on the relationship between the brain structural changes and Aβ positivity rather than the cognitive levels. However, if Aβ positivity and cognitive levels are predicted together, these features need to be considered as well.

Our study showed that L-ERC thickness is an important ROI for the classification of Aβ+ samples in the XGBoost method and that it significantly differed depending on the accumulation of Aβ even in the same diagnosis categories. ERC is known to play an essential role in memory formation and is one of the first affected areas in AD because of its connection to the hippocampus and neocortex [31,32], and ERC thickness is associated with MMSE and AD assessment scale–cognitive [33]. Previous studies have even shown that ERC is a more important biomarker than the hippocampus in detecting a conversion from non-dementia in patients to AD or from MCI to AD [34-36]. In addition, ERC thickness is an important ROI in distinguishing AD and healthy controls [37].

14681331, ja, Downloaded from https://onlinelibrary.wiley.com/doi/10.1111/ene.15775 by University Of Southern California, Wiley Online Library on [27/03/2023]. See the Terms and Conditions (https://onlinelibrary.wiley.com/terms-and-conditions) on Wiley Online Library for rules of use; OA articles are governed by the applicable Creative Commons License

For the relationship between cortical thickness and Aβ positivity, an early study reported that there was no significant difference between Aβ+ (nine samples) and Aβ- (35 samples) in medial temporal lobe cortex thickness [38]. However, this observation might be due to the small number of samples in the study. In our study, we observed in the NC diagnosis category of the EW cohort (Table 4) that the five ROIs showed p-values > 0.05 and L-ERC thickness had the p-value of 0.052, where the number of NC subjects was small with five Aβ+ and 37 Aβ- samples. When the ADNI cohort with the larger number of samples was used, four ROIs including ERC showed p-values < 0.05 even in the NC category. In addition, several studies showed that ERC thickness declined in Aβ+ samples [39,40].

A recent study has shown that APOE4 expression affects the regulation of lipid metabolism in the ERC, implying that APOE4 increases the susceptibility of neurons in the ERC to AD pathogenesis [41]. This previous study supports our results that Aβ classification performance was improved when APOE and sMRI were combined, and that L-ERC thickness and APOE genotype were significantly related to one another.

In addition to L-ERC thickness, Table 4 shows a significant difference between Aβ+ and Aβ- samples in medial orbitofrontal cortex (mOFC) thickness, except for that of dementia in the ADNI cohort. Several studies suggested that mOFC is associated with Aβ accumulation in an early stage of AD [42,43]. By analyzing the ADNI cohort, Palmqvist et al. [42] showed that Aβ accumulation starts in the core regions of the default mode network, including mOFC. Our results also support that mOFC is an important region for distinguishing Aβ positivity in our EW cohort.

As progression of MCI to AD is clinically important, several studies have been conducted to predict the conversion of MCI to AD using sMRI [44,45]. Most studies used the ADNI cohort as it contains longitudinal data. Thus, by following up with subjects in the EW cohort, we will further investigate longitudinal changes on the relationship between ROIs in brain and Aβ accumulation and develop computational models to predict the conversion of MCI to AD as future work.

Accepted Article

14681331, ja, Downloaded from https://onlinelibrary.wiley.com/doi/10.1111/ene.15775 by University Of Southern California, Wiley Online Library on [27/03/2023]. See the Terms and Conditions (https://onlinelibrary.wiley.com/terms-and-conditions) on Wiley Online Library for rules of use; OA articles are governed by the applicable Creative Commons License

Accepted Article

## AUTHOR CONTRIBUTIONS

HL and JJ initiated and supervised the project. JJ, HP, JY, and JH collected data. HL and JH developed the algorithm and analyzed the results. HL, JJ, HP, and JH wrote the manuscript. JH performed computational experiments

## ACKNOWLEDGMENTS

Data collection and sharing for this project was funded by the Alzheimer's Disease Neuroimaging Initiative (ADNI) (National Institutes of Health Grant U01 AG024904) and DOD-ADNI (Department of Defense award number W81XWH-12-2-0012). ADNI is funded by the National Institute on Aging, the National Institute of Biomedical Imaging and Bioengineering, and through generous contributions from AbbVie, Alzheimer's Association; Alzheimer's Drug Discovery Foundation; Araclon Biotech; BioClinica, Inc.; Biogen; Bristol-Myers Squibb Company; CereSpir, Inc.; Cogstate; Eisai Inc.; Elan Pharmaceuticals, Inc.; Eli Lilly and Company; EuroImmun; F. Hoffmann-La Roche Ltd and its affiliated company Genentech, Inc.; Fujirebio; GE Healthcare; IXICO Ltd.; Janssen Alzheimer Immunotherapy Research & Development, LLC.; Johnson & Johnson Pharmaceutical Research & Development LLC.; Lumosity; Lundbeck; Merck & Co., Inc.;Meso Scale Diagnostics, LLC.; NeuroRx Research; Neurotrack Technologies; Novartis Pharmaceuticals Corporation; Pfizer Inc.; Piramal Imaging; Servier; Takeda Pharmaceutical Company; and Transition Therapeutics. The Canadian Institute of Health Research is providing funds to support the ADNI clinical sites in Canada. Private sector contributions are facilitated by the Foundation for the National Institutes of Health (www.fnih.org). The grantee organization is the Northern California Institute for Research and Education, and the study was coordinated by the Alzheimer's Therapeutic Research Institute at the University of Southern California. ADNI data were disseminated by the Laboratory for Neuroimaging at the University of Southern California.

## CONFLICT OF INTEREST

The authors declare that there are no conflicts of interest associated with this work.

## DATA AVAILABILITY STATEMENT

Data on the Ewha Womans cohort are available upon request.

## SUPPORTING INFORMATION

Additional supporting information may be found online in the Supporting Information section at the end of the article.

14681331, ja, Downloaded from https://onlinelibrary.wiley.com/doi/10.1111/ene.15775 by University Of Southern California, Wiley Online Library on [27/03/2023]. See the Terms and Conditions (https://onlinelibrary.wiley.com/terms-and-conditions) on Wiley Online Library for rules of use; OA articles are governed by the applicable Creative Commons License

Accepted Article

## REFERENCES


1. Health NCCfM, Britain G. *Dementia: The NICE-SCIE Guideline on Supporting People with Dementia and Their Carers in Health and Social Care*. British Psychological Society and Royal College of Psychiatrists; 2007.
2. 2022 Alzheimer's disease facts and figures. *Alzheimers Dement*. Apr 2022;18(4):700-789. doi:10.1002/alz.12638
3. Rajan KB, Weuve J, Barnes LL, Wilson RS, Evans DA. Prevalence and incidence of clinically diagnosed Alzheimer's disease dementia from 1994 to 2012 in a population study. *Alzheimers Dement*. Jan 2019;15(1):1-7. doi:10.1016/j.jalz.2018.07.216
4. Chen G-f, Xu T-h, Yan Y, et al. Amyloid beta: structure, biology and structure-based therapeutic development. *Acta Pharmacologica Sinica*. 2017;38(9):1205-1235.
5. Lee JC, Kim SJ, Hong S, Kim Y. Diagnosis of Alzheimer's disease utilizing amyloid and tau as fluid biomarkers. *Experimental & molecular medicine*. 2019;51(5):1-10.
6. Johnson KA, Sperling RA, Gidicsin CM, et al. Florbetapir (F18-AV-45) PET to assess amyloid burden in Alzheimer's disease dementia, mild cognitive impairment, and normal aging. *Alzheimer's & Dementia*. 2013;9(5):S72-S83.
7. Camus V, Payoux P, Barré L, et al. Using PET with 18F-AV-45 (florbetapir) to quantify brain amyloid load in a clinical environment. *European journal of nuclear medicine and molecular imaging*. 2012;39(4):621-631.
8. Rowe CC, Ackerman U, Browne W, et al. Imaging of amyloid β in Alzheimer's disease with 18F-BAY94-9172, a novel PET tracer: proof of mechanism. *The Lancet Neurology*. 2008;7(2):129-135.
9. Thal DR, Beach TG, Zanette M, et al. [18F] flutemetamol amyloid positron emission tomography in preclinical and symptomatic Alzheimer's disease: specific detection of advanced phases of amyloid-β pathology. *Alzheimer's & Dementia*. 2015;11(8):975-985.
10. Pannee J, Portelius E, Minthon L, et al. Reference measurement procedure for CSF amyloid beta (Aβ) 1–42 and the CSF Aβ1–42/Aβ1–40 ratio–a cross-validation study against amyloid PET. *Journal of neurochemistry*. 2016;139(4):651-658.
11. Tosun D, Chen Y-F, Yu P, et al. Amyloid status imputed from a multimodal classifier including structural MRI distinguishes progressors from nonprogressors in a mild Alzheimer's disease clinical trial cohort. *Alzheimer's & Dementia*. 2016;12(9):977-986.
12. Tosun D, Joshi S, Weiner MW, Initiative AsDN. Neuroimaging predictors of brain amyloidosis in mild cognitive impairment. *Annals of neurology*. 2013;74(2):188-198.
13. Jack Jr CR, Bernstein MA, Fox NC, et al. The Alzheimer's disease neuroimaging initiative (ADNI): MRI methods. *Journal of Magnetic Resonance Imaging: An Official Journal of the International Society for Magnetic Resonance in Medicine*. 2008;27(4):685-691.
14. Altmann A, Toloşi L, Sander O, Lengauer T. Permutation importance: a corrected feature importance measure. *Bioinformatics*. 2010;26(10):1340-1347.
15. Jack Jr CR, Bennett DA, Blennow K, et al. NIA-AA research framework: toward a biological definition of Alzheimer's disease. *Alzheimer's & Dementia*. 2018;14(4):535-562.
16. Han C, Jo SA, Jo I, Kim E, Park MH, Kang Y. An adaptation of the Korean mini-mental state examination (K-MMSE) in elderly Koreans: demographic influence and population-based norms (the AGE study). *Archives of gerontology and geriatrics*. 2008;47(3):302-310.
17. Ysj K, Dl N. Seoul Neuropsychological Screening Battery (SNSB-II). Seoul: Human Brain Research & Consulting Co; 2012.


14681331, ja, Downloaded from https://onlinelibrary.wiley.com/doi/10.1111/ene.15775 by University Of Southern California, Wiley Online Library on [27/03/2023]. See the Terms and Conditions (https://onlinelibrary.wiley.com/terms-and-conditions) on Wiley Online Library for rules of use; OA articles are governed by the applicable Creative Commons License

Accepted Article

18. Barthel H, Gertz H-J, Dresel S, et al. Cerebral amyloid-β PET with florbetaben (18F) in patients with Alzheimer's disease and healthy controls: a multicentre phase 2 diagnostic study. *The Lancet Neurology*. 2011;10(5):424-435.
19. Bullich S, Seibyl J, Catafau AM, et al. Optimized classification of 18F-Florbetaben PET scans as positive and negative using an SUVR quantitative approach and comparison to visual assessment. *NeuroImage: Clinical*. 2017;15:325-332.
20. Landau S, Jagust W. Florbetapir processing methods. *Los Angeles: Alzheimer's Disease Neuroimaging Institute*. 2015;
21. Dukart J, Mueller K, Villringer A, et al. Relationship between imaging biomarkers, age, progression and symptom severity in Alzheimer's disease. *NeuroImage: Clinical*. 2013;3:84-94.
22. Tyas SL, Manfreda J, Strain LA, Montgomery PR. Risk factors for Alzheimer's disease: a population-based, longitudinal study in Manitoba, Canada. *International journal of epidemiology*. 2001;30(3):590-597.
23. Zhou T, Thung KH, Zhu X, Shen D. Effective feature learning and fusion of multimodality data using stage-wise deep neural network for dementia diagnosis. *Human brain mapping*. 2019;40(3):1001-1016.
24. McCullagh P, Nelder JA. *Generalized linear models*. Routledge; 2019.
25. Dorey E, Chang N, Liu QY, Yang Z, Zhang W. Apolipoprotein E, amyloid-beta, and neuroinflammation in Alzheimer's disease. *Neuroscience bulletin*. 2014;30(2):317-330.
26. Schmechel D, Saunders A, Strittmatter W, et al. Increased amyloid beta-peptide deposition in cerebral cortex as a consequence of apolipoprotein E genotype in late-onset Alzheimer disease. *Proceedings of the National Academy of Sciences*. 1993;90(20):9649-9653.
27. Morris JC, Roe CM, Xiong C, et al. APOE predicts amyloid-beta but not tau Alzheimer pathology in cognitively normal aging. *Annals of neurology*. 2010;67(1):122-131.
28. Seripa D, D'Onofrio G, Panza F, Cascavilla L, Masullo C, Pilotto A. The genetics of the human APOE polymorphism. *Rejuvenation research*. 2011;14(5):491-500.
29. Chen T, He T, Benesty M, et al. Xgboost: extreme gradient boosting. *R package version 04-2*. 2015;1(4):1-4.
30. Boughorbel S, Jarray F, El-Anbari M. Optimal classifier for imbalanced data using Matthews Correlation Coefficient metric. *PloS one*. 2017;12(6):e0177678.
31. Thaker AA, Weinberg BD, Dillon WP, et al. Entorhinal cortex: antemortem cortical thickness and postmortem neurofibrillary tangles and amyloid pathology. *American journal of neuroradiology*. 2017;38(5):961-965.
32. Squire LR, Zola-Morgan S. The medial temporal lobe memory system. *Science*. 1991;253(5026):1380-1386.
33. Velayudhan L, Proitsi P, Westman E, et al. Entorhinal cortex thickness predicts cognitive decline in Alzheimer's disease. *Journal of Alzheimer's Disease*. 2013;33(3):755-766.
34. Killiany R, Hyman B, Gomez-Isla T, et al. MRI measures of entorhinal cortex vs hippocampus in preclinical AD. *Neurology*. 2002;58(8):1188-1196.
35. Dickerson BC, Goncharova I, Sullivan M, et al. MRI-derived entorhinal and hippocampal atrophy in incipient and very mild Alzheimer's disease. *Neurobiology of aging*. 2001;22(5):747-754.
36. Du A, Schuff N, Amend D, et al. Magnetic resonance imaging of the entorhinal cortex and hippocampus in mild cognitive impairment and Alzheimer's disease. *Journal of Neurology, Neurosurgery & Psychiatry*. 2001;71(4):441-447.

14681331, ja, Downloaded from https://onlinelibrary.wiley.com/doi/10.1111/ene.15775 by University Of Southern California, Wiley Online Library on [27/03/2023]. See the Terms and Conditions (https://onlinelibrary.wiley.com/terms-and-conditions) on Wiley Online Library for rules of use; OA articles are governed by the applicable Creative Commons License

37. Cho Y, Seong J-K, Jeong Y, Shin SY, Initiative AsDN. Individual subject classification for Alzheimer's disease based on incremental learning using a spatial frequency representation of cortical thickness data. *Neuroimage*. 2012;59(3):2217-2230.
38. Dickerson BC, Bakkour A, Salat DH, et al. The cortical signature of Alzheimer's disease: regionally specific cortical thinning relates to symptom severity in very mild to mild AD dementia and is detectable in asymptomatic amyloid-positive individuals. *Cerebral cortex*. 2009;19(3):497-510.
39. Doherty BM, Schultz SA, Oh JM, et al. Amyloid burden, cortical thickness, and cognitive function in the Wisconsin Registry for Alzheimer's Prevention. *Alzheimer's & dementia: diagnosis, assessment & disease monitoring*. 2015;1(2):160-169.
40. Morar U, Izquierdo W, Martin H, et al. A study of the longitudinal changes in multiple cerebrospinal fluid and volumetric magnetic resonance imaging biomarkers on converter and non-converter Alzheimer's disease subjects with consideration for their amyloid beta status. *Alzheimer's & Dementia: Diagnosis, Assessment & Disease Monitoring*. 2022;14(1):e12258.
41. Miranda AM, Ashok A, Chan RB, et al. Effects of APOE4 allelic dosage on lipidomic signatures in the entorhinal cortex of aged mice. *Translational psychiatry*. 2022;12(1):1-10.
42. Palmqvist S, Schöll M, Strandberg O, et al. Earliest accumulation of β-amyloid occurs within the default-mode network and concurrently affects brain connectivity. *Nature communications*. 2017;8(1):1-13.
43. Sepulcre J, Sabuncu MR, Becker A, Sperling R, Johnson KA. In vivo characterization of the early states of the amyloid-beta network. *Brain*. 2013;136(7):2239-2252.
44. Nakagawa T, Ishida M, Naito J, et al. Prediction of conversion to Alzheimer's disease using deep survival analysis of MRI images. *Brain communications*. 2020;2(1):fcaa057.
45. Long X, Chen L, Jiang C, Zhang L, Initiative AsDN. Prediction and classification of Alzheimer disease based on quantification of MRI deformation. *PloS one*. 2017;12(3):e0173372.

Accepted Article

14681331, ja, Downloaded from https://onlinelibrary.wiley.com/doi/10.1111/ene.15775 by University Of Southern California, Wiley Online Library on [27/03/2023]. See the Terms and Conditions (https://onlinelibrary.wiley.com/terms-and-conditions) on Wiley Online Library for rules of use; OA articles are governed by the applicable Creative Commons License